

Sub-mm Singledish and Interferometric Observations of the Proto-cluster around 4C 23.56 at $z = 2.5$

K. SUZUKI¹, K. KOHNO^{1,2}, I. TANAKA³, T. KODAMA⁴, B. HATSUKADE⁵, Y. TAMURA¹,
K. NAKANISHI^{4,6,7}, D. IONO⁸, M. KAJISAWA⁹, S. IKARASHI¹, H. UMEHATA¹, R. IVISON¹⁰,
G. WILSON¹¹, M. S. YUN¹¹, D. HUGHES¹², I. ARETXAGA¹², M. ZEBALLOS¹²

¹Institute of Astronomy, University of Tokyo, kenta_suzuki@ioa.s.u-tokyo.ac.jp, ²Research Center for the Early Universe, University of Tokyo, ³Subaru Telescope, National Astronomical Observatory of Japan, ⁴National Astronomical Observatory of Japan, ⁵Department of Astronomy, Kyoto University, ⁶The Graduate University for Advanced Studies, ⁷Joint ALMA Observatory, ⁸Nobeyama Radio Observatory, ⁹Research Center for Space and Cosmic Evolution, Ehime University, ¹⁰UK Astronomy Technology Centre, Science and Technology Facilities Council, Royal Observatory, ¹¹Department of Astronomy, University of Massachusetts, ¹²Instituto Nacional de Astrofísica, Óptica y Electrónica,

The proto-cluster around the radio galaxy 4C 23.56 at $z = 2.48$ is known as an overdense region of bright H α emitters (HAEs) with their star formation rates (SFRs) \sim a few $100 M_{\odot} \text{ yr}^{-1}$, investigated by MOIRCS/SUBARU narrow band survey. This region should be the best site to study formation history of cluster massive galaxies at the early universe. We conducted AzTEC / ASTE deep 1.1 mm continuum survey toward this region. It covers $\sim 166 \text{ arcmin}^2$ wide area with $1\sigma = 0.6 - 0.9 \text{ mJy beam}^{-1}$. We robustly detect 35 of 1.1 mm sources with $3.5 - 16.7\sigma$ within the survey field. These sources have $L_{\text{FIR}} \sim 3.0 \times 10^{12} - 2.0 \times 10^{13} L_{\odot}$ and SFRs $\sim 520 - 3380 M_{\odot} \text{ yr}^{-1}$ on some uncertainties of dust parameters and redshifts. We find a remarkable spatial coincidence between 1.1 mm sources and bright HAEs in $2 \times 2 \text{ arcmin}^2$ or $\sim 3 \text{ Mpc}$ scale. IRAC colors of HAEs are also consistent with that of SMGs at $z \sim 2.5$, implying that some 1.1 mm sources in this protocluster with SFR $\sim 1000 M_{\odot} \text{ yr}^{-1}$ are superposition of dusty HAEs with SFR \sim a few $100 M_{\odot} \text{ yr}^{-1}$. We successively conducted Plateau de Bure Interferometer (PdBI) follow up observation for dust continuum and CO(5-4) at 165 GHz. We detected 1.8 mm PdBI sources at the peak of each AzTEC sources. We also detected a CO(5-4) source which is identified with a HAE. The CO(5-4) emission shows a broad line shape (full width $\sim 1000 \text{ km s}^{-1}$), implying that this could be a multiple or merging system. The detected CO(5-4) luminosity corresponds to the molecular gas mass of $2.9 \times 10^{10} M_{\odot}$ assuming ULIRG-like CO-to-H $_2$ conversion factor. This results in a star formation efficiency (SFE) $\equiv L_{\text{IR}} / L'_{\text{CO}}$ of $144 L_{\odot} (\text{K km s}^{-1} \text{ pc}^2)^{-1}$, suggesting that this HAE shows an intermediate SFE between quasars/SMGs (“starburst sequence”) and gas-rich star-forming galaxies (i.e., “disk-mode sequence”).

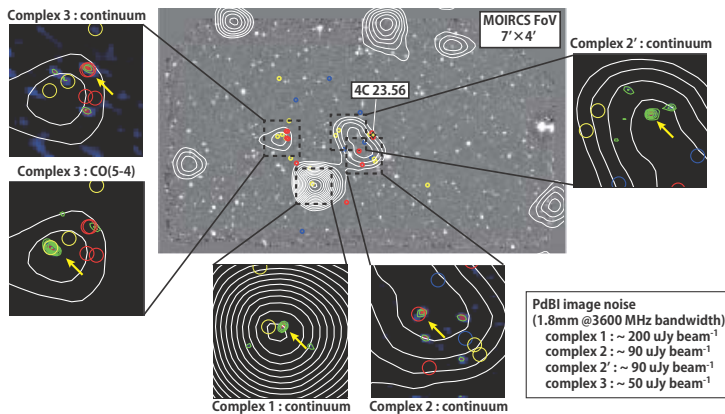


Figure 1: The spatial distributions of HAEs (circles with colors, red : SFR $> 150 M_{\odot} \text{ yr}^{-1}$, yellow ; $50 M_{\odot} \text{ yr}^{-1} < \text{SFR} < 150 M_{\odot} \text{ yr}^{-1}$, blue ; $20 M_{\odot} \text{ yr}^{-1} < \text{SFR} < 50 M_{\odot} \text{ yr}^{-1}$, respectively.), AzTEC 1.1 mm sources (white contours, 1σ steps from 3.5σ). Close up PdBI 1.8 mm continuum and CO(5-4) images (green contours, 1σ steps from 3σ) for 4 complexes are also shown (Suzuki et al. 2012).

Sub-millimetre galaxies in cosmological hydrodynamic simulations: Source number counts and the spatial clusteringIKKOH SHIMIZU¹¹ Osaka Sangyo University, Japan.

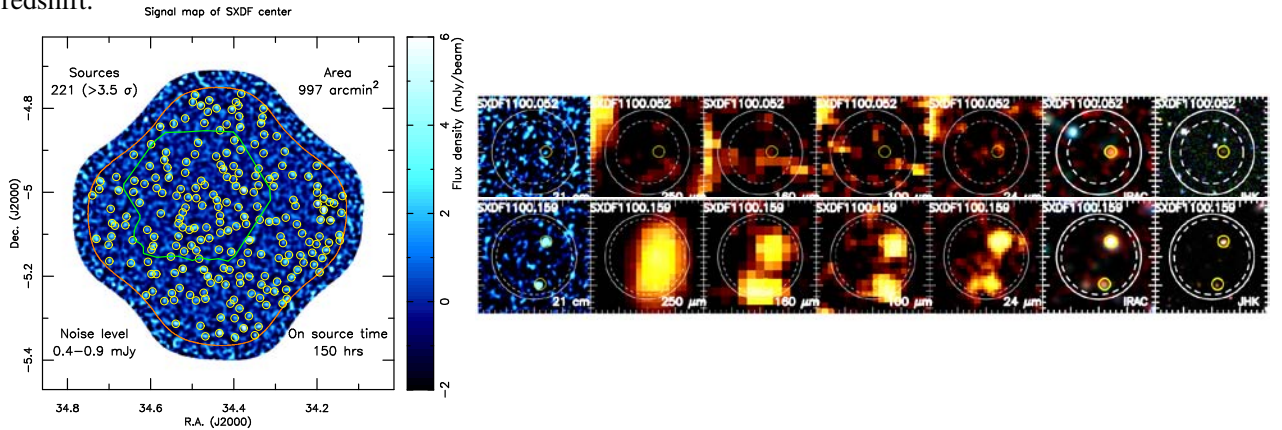
We use large cosmological Smoothed-Particle-Hydrodynamics simulations to study the formation and evolution of sub-millimetre galaxies (SMGs). In our previous work, we studied the statistical properties of ultra-violet selected star-forming galaxies at high redshifts. We populate the same cosmological simulations with SMGs by calculating the reprocess of stellar light by dust grains into far-infrared to millimetre wavebands in a self-consistent manner. We generate light-cone outputs to compare directly the statistical properties of the simulated SMGs with available observations. Our model reproduces the submm source number counts and the clustering amplitude. We show that bright SMGs with flux $S > 1$ mJy reside in halos with mass of $\sim 10^{13} M_{\odot}$ and have stellar masses greater than $10^{11} M_{\odot}$. The angular cross-correlation between the SMGs and Lyman- α emitters is significantly weaker than that between the SMGs and Lyman-break galaxies. The cross-correlation is also weaker than the auto-correlation of the SMGs. The redshift distribution of the SMGs shows a broad peak at $z \sim 2$, where Bright SMGs contribute significantly to the global cosmic star formation rate density. Our model predicts that there are hundreds of SMGs with $S > 0.1$ mJy at $z > 5$ per 1 square degree field. Such SMGs can be detected by ALMA.

AzTEC/ASTE deep and wide submillimeter galaxy survey in the Subaru/XMM-Newton Deep Field: Identification of VLA, Spitzer and Herschel counterparts to 1100- μm -selected galaxies and redshifts

S. IKARASHI¹, K. KOHNO¹, I. ARETXAGA², V. ARUMUGAM³, K. CAPUTI⁴, J. DUNLOP³, B. HATSUKADE⁵, D. HUGHES², D. IONO⁶, R. IVISON³, R. KAWABE⁷, K. MOTOHARA¹, K. NAKANISHI⁷, K. OHTA⁵, K. SUZUKI¹, Y. TAMURA¹, H. UMEHATA¹, G. WILSON⁸, K. YABE⁹, M. YUN⁸

¹ Institute of Astronomy, University of Tokyo, Japan, ² Instituto Nacional de Astrofísica, Óptica y Electrónica (INAOE), Mexico, ³ Institute for Astronomy, University of Edinburgh, Royal Observatory, UK, ⁴ Kapteyn Astronomical Institute, University of Groningen, Netherlands, ⁵ Kyoto University, Japan, ⁶ Nobeyama Radio Observatory, Japan, ⁷ ALMA Project Office, National Astronomical Observatory, Japan, ⁸ Department of Astronomy, University of Massachusetts, USA, ⁹ National Astronomical Observatory, Japan

We present results of our AzTEC/ASTE submillimeter galaxies (SMGs) survey in the Subaru/XMM-Newton Deep Field (SXDF), and VLA (21 cm), *Spitzer* (3.6-8 μm and 24 μm) and *Herschel* (100 and 160 μm) counterpart identifications to 1100- μm -selected SMGs. We obtained a 1100- μm map of 997 arcmin² with the rms noise level of ~ 0.5 mJy (1 σ). Our AzTEC map achieved new detections of 221 sources ($S/N \geq 3.5 \sigma$). Deep *Herschel* PACS 100- μm and 160- μm images cover the whole of the AzTEC map, and 34 of 221 (= 15 %) and 54 of 221 (= 24 %) AzTEC sources have PACS 100- μm and 160- μm counterparts, respectively. We found VLA radio and/or MIPS 24- μm robust (with a significance of ≥ 95 %) counterparts to 102 of 221 the AzTEC SMGs. In addition to this, we have developed an improved identification method using IRAC data (3.6-8 μm) and their colors, in order to cover the AzTEC SMGs located at higher redshift such as $z > 3$, which is inaccessible with the existing VLA, MIPS and *Herschel* data alone. With this method, we have achieved another robust detections of 20 IRAC counterparts to AzTEC sources. 131 of 221 AzTEC sources have at least one robust counterparts, and 23 of 221 have more than two robust counterparts. Including tentative identifications (with a significance of ≥ 90 %), 164 of 221 (= 74 %) 1100- μm -selected SMGs have counterparts. We estimated photometric redshifts of the counterparts using deep near-, and med-infrared and optical data, providing z_{median} of 2.2. Among them, we found that there were some 1100- μm sources faint in multi-bands data suggesting the extremely high redshift.



(Left) AzTEC 1100- μm map of SXDF. The coverage of useful AzTEC/ASTE data is enclosed by orange solid line. The yellow circles show the positions of the detected AzTEC source. Green line shows the area covered by SCUBA in SHADES surveys (e.g., Coppin et al. 2006). (Right) Multi-wavelength images of AzTEC SMGs. Here, representative 2 targets are shown. From left to right: VLA, SPIRE, PACS, MIPS and IRAC images. Solid large white circles indicate the beam size of AzTEC/ASTE (30'') and dashed white circles show the 2σ position error on the AzTEC source. Solid yellow lines show the positions of the robust counterparts.

Clustering Properties of 1.1 mm-selected Submillimetre Galaxies Uncovered by AzTEC Deep Surveys

B. HATSUKADE¹ ET AL.

¹ Department of Astronomy, Kyoto University, Kyoto 606-8502, Japan.

Millimetre/submillimetre-bright galaxy population (SMGs) are dusty starburst galaxies with star-formation rates (SFRs) of $\sim 1000 M_{\odot} \text{ yr}^{-1}$ at high redshifts ($z > 1$). While it is thought that SMGs may be the progenitors of massive elliptical galaxies in the present-day universe observed during their peak phase of stellar mass buildup, the evolutionary history of SMGs and their relationship to other galaxy populations at high-redshift and in the local universe are still uncertain.

We performed deep and wide-field surveys at 1.1 mm using AzTEC camera mounted on ASTE. We calculate the two-point angular autocorrelation functions in seven deep survey fields: AKARI Deep Field South (ADF-S), COSMOS, GOODS-S, Lockman Hole East, SSA 22, and SXDF. We detect evidence for clustering signals in all the fields. By averaging the results on the bright sources measured in the ADF-S, the SSA 22, and the SXDF fields, we derived a more significant correlation function of 1.1 mm sources. The correlation length for the combined data is estimated to be $r_0 = 13_{-6}^{+4} h^{-1}$ Mpc by assuming a Gaussian redshift distribution centered at $z = 2.5$ with a standard deviation of $\sigma_z = 0.5$. A comparison of the correlation length with a bias evolution model of dark halos suggests that dark halos hosting bright 1.1 mm sources evolve into galaxy clusters in the present-day universe. In this scenario, the 1.1 mm sources residing in the dark halos evolve into massive galaxies located in the clusters.

Submillimeter Galaxies in the SSA22 Protocluster at $z=3.1$

H.UMEHATA¹, Y.TAMURA¹, K.KOHNO¹, S.IKARASHI¹, K.SUZUKI¹, D.IONO², T.TAKATA²,
K.NAKANISHI², Y.MATSUDA², R.KAWAVE², B.HATSUKADE³, T.YAMADA⁴, R.IVISON⁵, M.YUN⁶,
G.WILSON⁶, D.HUGHES⁷

¹ The University of Tokyo, Japan.

² National Astronomical Observatory of Japan

³ Kyoto University, Japan

⁴ Tohoku Univeristy, Japan

⁵ Institute for Astronomy, University of Edinburgh, Royal Observatory, UK

⁶ Department of Astronomy, University of Massachusetts, USA

⁷ Instituto Nacional de Astrofísica, Óptica y Electrónica (INAOE), Mexico

We present the results of counterpart identification of submillimeter galaxies (SMGs) detected in the SSA22 protocluster, which is traced by Ly α emitting galaxies (LAEs) at $z = 3.1$. 112 SMGs were uncovered in this field with a signal to noise ratio of > 3.5 by a 1.1mm deep extragalactic survey with AzTEC camera mounted on the Atacama Submillimeter Telescope Experiment (ASTE). We searched counterparts for these 1.1mm selected SMGs using the following three methods; radio(1.4GHz), MIPS ch1($24\mu\text{m}$), and IRAC color($3.6\mu\text{m}$, $4.5\mu\text{m}$, $5.8\mu\text{m}$, and $8.0\mu\text{m}$) diagnostics. As a result we identified 48 SMGs with at least one counterpart. Furthermore we extract 34 SMGs from those with counterpart and observed by IRAC 4 channels and derive their photometric redshifts with photometric data from optical to mid-infrared wavelength (at most 13 bands). Finally we identify seven SMGs as reliable candidates of $z=3.1$ protocluster member. Two point angular correlation function between LAEs and these SMGs shows that there are significant spatial correlation, which indicates SMGs are correlated with the large scale structure. These results indicate that high density regions at the high redshift universe are the site of SMG formation. This picture is consistent with predictions from the standard model of hierarchical structure formation. We also detect luminous X-ray emission ($L_{X0.5-8.0\text{keV}} \sim 10^{44} \text{ ergs s}^{-1}$) in three SMGs around the core of the protocluster, suggesting that these harbor luminous AGNs and are at the terminal stage of starbursts.

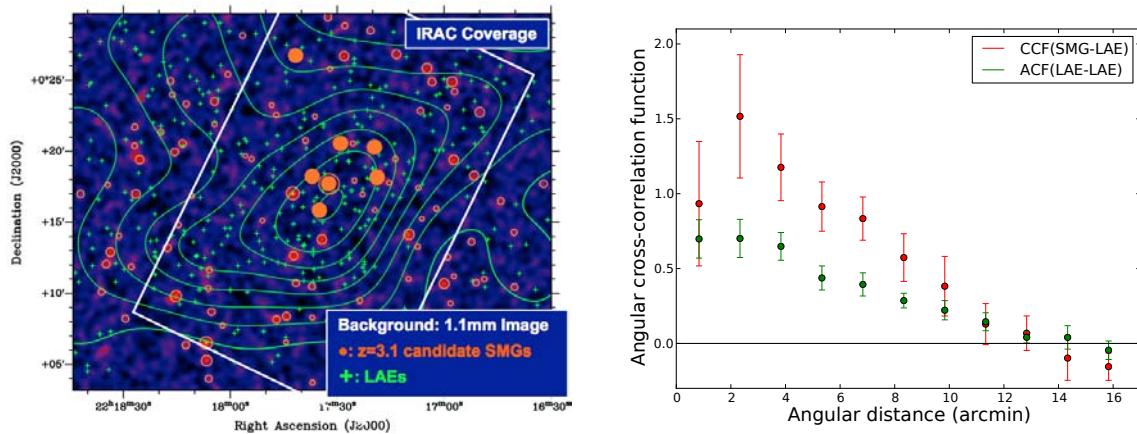


Figure1: (left) Sky distribution of SMGs. (right) Angular cross-correlation function between $z = 3.1$ candidate SMGs and LAEs.

References:

Tamura et al. 2009, Nature, 459, 61

CO Observations of Distant Bright Galaxies at the 45mD. IONO¹, B. HATSUKADE², K. KOHNO³, R. KAWABE⁴ AND THE HIGH-Z LEGACY TEAM¹ Chile Observatory, NAOJ, Tokyo, Japan.² Kyoto University, Kyoto, Japan.³ University of Tokyo, Tokyo, Japan.⁴ Joint ALMA Observatory, Santiago, Chile.

We present initial results from the CO survey toward high redshift galaxies using the Nobeyama 45m telescope. Using the new wide bandwidth spectrometer equipped with a two-beam SIS receiver, we have robust new detections of three high redshift ($z = 1.6 - 3.4$) submillimeter galaxies (SXDF 1100.001, SDP9, and SDP17), one tentative detection (SDSS J160705+533558), and one non-detection (COSMOS-AzTEC1). The galaxies observed during the commissioning phase are sources with known spectroscopic redshifts from previous optical or from wide-band submm spectroscopy. The derived molecular gas mass and line widths from Gaussian fits are $\sim 10^{11} M_{\odot}$ and 430 — 530 km/s, which are consistent with previous CO observations of distant submm galaxies and quasars. The spectrometer that allows a maximum of 32 GHz instantaneous bandwidth will provide new science capabilities at the Nobeyama 45m telescope, allowing us to determine redshifts of bright submm selected galaxies without any prior redshift information.

Tilted Cosmological Model With Barotropic Fluid DistributionRakeshwar Purohit¹ and Anita Bagora(Menaria)^{2*}¹ *Department of Mathematics, M.L. Sukhadia University, Udaipur-313001, India,*² *Department of Mathematics, Jaipur National University, Jaipur-302027, India,*

Abstract. We investigated tilted Bianchi type I cosmological model for barotropic fluid ($p = \gamma\rho$), where p being isotropic pressure, ρ the matter density with $0 \leq \gamma \leq 1$. To determine the complete solution, we have assumed the relation between metric potential as $A=BC$. To get model in terms of cosmic time t , we have also assumed some special condition. The physical and geometrical aspects of both the model are discussed.

Keywords: Cosmology, Tilted cosmological model, Bianchi type-I universe, Barotropic fluid.

PACS numbers: 98.80.-k, 04.20.-q;

*corresponding author.

Molecular gas properties and star formation in interacting galaxies

H. KANEKO¹, K. NARIO^{2,3}, D. IONO^{3,4}, Y. TAMURA⁵, T. TOMOKA⁶, K. NAKANISHI^{2,4,7} AND T. SAWADA^{4,7}

¹ University of Tsukuba

² The Graduate University for Advanced Studies ³ Nobeyama Radio Observatory ⁴ National Astronomical Observatory of Japan ⁵ The University of Tokyo ⁶ Joetsu University of Education ⁷ Joint ALMA Observatory

Galaxy encounters (e.g., collisions and mergers) play important roles for evolution of galaxies. Close galaxy-galaxy interactions greatly alter the distribution and kinematics of star and gas. During this phenomena, a significant enhancement of star formation is observed (Bushouse 1986). It is also known that the star formation activity follows evolution phases of interacting galaxies (hereafter IGs). While in IGs in early stage which show weak morphological disturbance star formation rate (SFR) is only a few times higher than field galaxies, SFR reaches to a few 10 times higher than field galaxies at late stage where two nuclei merge (Kennicutt et al. 1987). Especially, ultra luminous infrared galaxies (ULIRGs: $L_{\text{IR}} > 10^{12} L_{\odot}$) most of which are thought to be in the late stage of the interaction (Clements et al. 1996) show bursts of star formation ($> 100 M_{\odot} \text{ yr}^{-1}$).

It is, however, still open question how star formation is activated in IGs. Since molecular gas is a fuel of star formation, it is important to investigate how the interaction affects on molecular gas properties. Previous CO observations have been mainly focused on ULIRGs which are thought to have large amount of molecular gas. In fact, Young & Scoville (1991) showed that IR luminous galaxies have molecular gas of more than $10^{10} M_{\odot}$. However, IGs in late stage like ULIRGs are not good for investigating the mechanism of active star formation in IGs because they already show burst of star formation. On the other hand, properties of molecular gas in IGs in earlier stage which will produce large amount of stars is not investigated well, since most CO observations are aimed at only the centre of galaxies.

We performed $^{12}\text{CO}(J = 1-0)$ OTF observations of four IGs in early and mid stage of interaction (Arp 84, VV 219, VV 254 and the Antennae Galaxies) using the 45-m telescope at Nobeyama Radio Observatory (Kaneko et al. submitted) and found the following facts.

The degree of the central concentration of molecular gas for IGs and isolated galaxies (data are taken from Nobeyama CO atlas, Kuno et al. 2007) are compared. In IGs the central concentration of molecular gas is lower than that in isolated galaxies. Taking account of results of the numerical simulations and the observations of galaxies in late stage, our results imply that central concentration of molecular gas decreases in the early stage at least once before falling into the nucleus.

We compared molecular gas fraction (f_{mol}), the fraction of molecular gas to total gas (defined as the sum of molecular hydrogen gas and atomic hydrogen gas) in IGs with isolated galaxies, and found that IGs have higher molecular fraction. From the theoretical model (Elmegreen 1993) fitting to the observed f_{mol} , we speculate that such high f_{mol} in IGs is due to external pressure and that the external pressure originates from the shocks induced by the interaction.

We assessed the relationship between molecular gas and star formation activity using star formation rate which is corrected dust extinction. No difference in Schmidt-Kennicutt relation is found between IGs in the early stage and isolated galaxies, although IGs have higher f_{mol} than isolated galaxies. On the other hand, IGs in the mid stage have higher SFE throughout the galaxies compared to those in the early stage.

References:

- Bushouse, H. A. 1986, AJ, 91, 255
- Clements, D. et al. 1996, MNRAS, 279, 477
- Kennicutt, R. C. Jr. et al. 1987, AJ, 93, 5
- Young, J. S. & Scoville, N. Z. 1991, ARA&A, 29, 581
- Kaneko, H. et al. submitted to PASJ
- Elmegreen, B. G. 1993, ApJ, 411, 170

Derivation of the Mass of Super-Massive Black Hole

KYOKO ONISHI¹, SATORU IGUCHI²

¹ Department of Astronomical Science, the Graduate University for Advanced Studies

² National Astronomical Observatory of Japan

We aim to establish a new method to derive the mass of Super Massive Black Hole (hereinafter SMBH; larger than $10^6 M_{\odot}$) in the center of the giant galaxies. The scientific importance of our study is:

- The determination of BH mass is fundamental to the field of black hole study; and
- This study suggests how SMBH and its host galaxy co-evolved, because the $M_{\text{BH}} - \sigma$ relation, where the σ is the central velocity dispersion of its host galaxy can be updated.

Our NMA and RAINBOW observation in 2004 was not able to derive a velocity distribution map at 100-pc scale of the molecular gas surrounding the central black hole of a giant radio galaxy. With high performances of ALMA, however, we can obtain a high-quality image with an angular resolution of 0.3 arcsec which is equivalent to 100 pc of this object. In the future, ALMA can achieve higher resolution of 0.01 arcsec that corresponds to 3 pc at the redshift of this object. We show the simulation results of several rotational models from our position-velocity map, and will present how the model coincides with the observed map.

Towards a Comprehensive Law of the Interstellar Medium

S. KOMUGI^{1,2}, R. MIURA², S. ONODERA³, N. KUNO⁴, T. TOMOKA⁵ ET AL.

¹ Joint ALMA Observatory

² Chile Observatory, National Astronomical Observatory of Japan ³ Meisei University ⁴ Nobeyama Radio Observatory, National Astronomical Observatory of Japan ⁵ Joetsu University of Education

Recent resolved observations of external galaxies have revealed that the relation between star formation rate and gas density breaks down at the scale of individual giant molecular clouds (GMCs). This shows that between individual GMCs, the interplay between the ISM and star formation is not expressible in terms of simple two-parameter laws like the Kennicutt-Schmidt law. Understanding the fundamental relation between various properties of GMCs and its environment is essential for gaining a comprehensive view of the ISM.

We have employed the Principal Component Analysis (PCA) approach to a catalogue of GMCs in the ultra-nearby galaxy M33 (Miura et al., submitted). By combining with the literature, we have compiled a large set of GMCs each with their size, line width, CO(J=3-2) luminosity, peak kinetic temperature, dust temperature, dust mass, K-band luminosity and star formation rate, along with the metallicity for a subset of sources. The GMCs are grouped by their type, a discrete measure of their evolutionary state. The PCA allows the derivation of the most fundamental relations between these parameters, while constructing a new set of orthogonal axes which describe the ISM better than the original parameters.

The most important relations derived from the PCA are found to include the equivalent of the Kennicutt-Schmidt (KS) relation and Larson's relation, as well as some other empirical relations which were previously unknown. In particular the KS relation includes parameters other than the CO luminosity and star formation rate, naturally revealing a new multi-parameter star formation law. Since these relations are constructed based on individual GMCs, the new relations are able to bridge between resolved and unresolved galaxies via spatial averaging. The PCA is also able to give actual values on the degree of importance of various physical parameters in these series of empirical laws.

I will review the process of the PCA, the results, and its future applications in the field of numerical simulations and interpretation of distant galaxies.

The Star Formation Law in Similar-Age Regions; Case Study of the Early-Phase Interacting Galaxy Taffy I

S. KOMUGI^{1,2}, K. TATEUCHI³, K. MOTOHARA³, T. TAKAGI⁴, D. IONO^{2,5}, H. KANEKO⁶, J. UEDA^{5,7},
T. R. SAITOH⁸ AND TAO/ANIR PROJECT TEAM.

¹ Joint ALMA Observatory

² Chile Observatory, National Astronomical Observatory of Japan ³ Institute of Astronomy, The University of Tokyo ⁴ Japan Aerospace Exploration Agency, Institute of Space and Astronautical Science

⁵ Nobeyama Radio Observatory, National Astronomical Observatory of Japan ⁶ Institute of Physics,

University of Tsukuba ⁷ Harvard-Smithsonian Center for Astrophysics ⁸ Interactive Research Center of Science, Tokyo Institute of Technology

In order to test a recent hypothesis that the dispersion in the Schmidt-Kennicutt law arises from variations in the evolutionary stage of star forming molecular clouds, we compared molecular gas and recent star formation in an early-phase merger galaxy pair, Taffy I (UGC 12915/UGC 12914, VV 254) which went through a direct collision 20 Myr ago and whose star forming regions are expected to have similar ages. Narrow-band Pa α image is obtained using the ANIR near-infrared camera on the mini-TAO 1m telescope. The image enables us to derive accurate star formation rates within the galaxy directly. The total star formation rate, 22.2 M $_{\odot}$ yr $^{-1}$, was found to be much higher than previous estimates. Ages of individual star forming blobs estimated from equivalent widths indicate that most star forming regions are 7 Myr old, except for a giant HII region at the bridge which is much younger. Comparison between star formation rates and molecular gas masses for the regions with the same age exhibits a surprisingly tight correlation, a slope of unity, and star formation efficiencies comparable to those of starburst galaxies. These results suggest that Taffy I has just evolved into a starburst system after the collision, and the star forming sites are at a similar stage in their evolution from natal molecular clouds except for the bridge region. The tight Schmidt-Kennicutt law supports the scenario that dispersion in the star formation law is in large part due to differences in evolutionary stage of star forming regions.

Microarcsecond structures of FSRQs 3C 279 and NRAO 530 revealed by Event Horizon Telescope observations

KAZUNORI AKIYAMA^{1,2}, RU-SEN LU³, VINCENT L. FISH³, SHEPERD S. DOELEMEN³, MAREKI HONMA^{2,4}, HIROSHI NAGAI² AND THE EVENT HORIZON TELESCOPE COLLABORATION

¹ The University of Tokyo

² National Astronomical Observatory of Japan

³ MIT Haystack observatory

⁴ The Graduate University for Advanced Studies

VLBI observations at short millimeter wavelengths (≤ 1.3 mm, ≥ 230 GHz) achieve extremely high-spatial resolution of tens of μas and enable direct studies on the nearby super massive black holes and the roots of relativistic jets in active galactic nuclei. Recently, the application of new technical developments and the appearance of new suitable antennas have established the technical feasibility of VLBI at such short mm-wavelengths with the Event Horizon Telescope (EHT; Doeleman et al. 2008, Fish et al. 2011). Here, we present the latest results of 1.3 mm VLBI observations in 2011 with the EHT towards the two well-known flat-spectrum radio quasars NRAO 530 and 3C 279.

3C 279 ($z=0.536$) is one of the most intensively studied blazars because of its remarkably strong variability in broad-band from radio to Gamma-ray and high optical polarization. On the other hand, NRAO 530 ($z=0.902$) is also known to be strongly variable at various wavelengths from radio to Gamma-ray. After the launch of Fermi, it underwent a GeV gamma-ray flare at the end of October, 2010 (D'Ammando & Vandenbroucke 2010). The extremely high resolution of the EHT enables us to explore inner-jet structures on a sub-pc scale that could give a clue for interpreting their broad-band variability.

We carried out 1.3 mm VLBI observations of 3C 279 and NRAO530 with the EHT in April 2011, 6 months after the above Gamma-ray flare on NRAO 530. In these observations, the 1.3 mm VLBI array consisted of three stations on Mauna Kea (SMA, JCMT and CSO) in Hawaii, the CARMA array in California and the AROSMT in Arizona, enabling us to sample visibilities from few $k\lambda$ to $\sim 3.5 G\lambda$. Strong fringe detections were made on both sources on all baselines. Furthermore, we robustly detected non-zero closure phases for both sources, indicating the presence of asymmetric compact structure. This is the second detection of closure phases in 1.3 mm VLBI observations.

In this talk, we report the first 1.3 mm VLBI models of 3C 279 and NRAO 530 using visibility amplitudes and closure phases. Then, we discuss relations between the models and multi-wavelength properties of these two sources. Finally, based on current EHT results, we discuss future possibilities for collaboration between the EHT including ASTE and the East Asia mm-VLBI network including VERA+KVN and the NRO 45m telescope.

References:

- D'Ammando, F., & Vandenbroucke, J. 2010, *The Astronomer's Telegram*, 3002, 1
 Doeleman, S.S., Weintraub, J., Rogers, A.E.E., et al. 2008, *Nature*, 455, 78
 Fish, V. L., Doeleman, S.S., Beaudoin, C., et al. 2011, *ApJL*, 727, L36

Detection of CO($J = 1 - 0$) Emission from Barred Spiral Galaxies at $z \sim 0.1$.

K. MATSUI¹, K. SORAI², Y. WATANABE³, N. KUNO⁴

¹ Nobeyama Radio Observatory, Japan.

² Hokkaido Univ., Japan.

³ Univ. of Tokyo, Japan.

⁴ Nobeyama Radio Observatory, Japan.

Bars in disk galaxies are thought to influence the evolution of disk galaxies through redistributing angular momentum among the galaxy components, such as stars, gas and dark matter, and transferring gas to the central kiloparsec regions. Previous studies have revealed that almost 70 % of disk galaxies in the local universe have bars in their inner regions. Furthermore Sheth et al. (2008, ApJ, 390, 426) showed that the fraction of the barred spiral galaxies among disk galaxies increases from $z \sim 0.8$ to date. It is important to study molecular gas properties of the barred spiral galaxies at intermediate redshift ($z \sim 0.1 - 1.0$) for studying their evolution, while there has been no observation toward the barred spiral galaxies in this redshift range.

We will present the results of CO ($J = 1 - 0$) observations toward nine barred spiral galaxies at $z = 0.08 - 0.25$ using the 45 m telescope at Nobeyama Radio Observatory. This survey is the first one specialized for barred spiral galaxies in this redshift range. We successfully detected CO emission from six galaxies out of nine, whose CO luminosity (L'_{CO}) ranges $(1.09 - 10.8) \times 10^9 \text{ K km s}^{-1} \text{ pc}^2$. These are the infrared (IR) dimmest galaxies that have ever been detected in CO at $z \sim 0.1$ to date. They follow the $L'_{\text{CO}} - L_{\text{IR}}$ relation among local spiral galaxies, Luminous Infrared Galaxies (LIRGs), Ultra-Luminous Infrared Galaxies (ULIRGs) and Sub-millimeter Galaxies (SMGs) as shown in figure a (from Matsui et al. 2012, PASJ, 64, 55). Their L'_{CO} and L_{IR} are higher than that of local spiral galaxies which have been detected in CO so far, and $L_{\text{IR}}/L'_{\text{CO}}$, which is a measure of star formation efficiency, is comparable to or slightly higher than that of local ones (see figure b). This result suggests that these galaxies are forming stars more actively than local spiral galaxies simply because they have more molecular gas as the fuel for star formation.

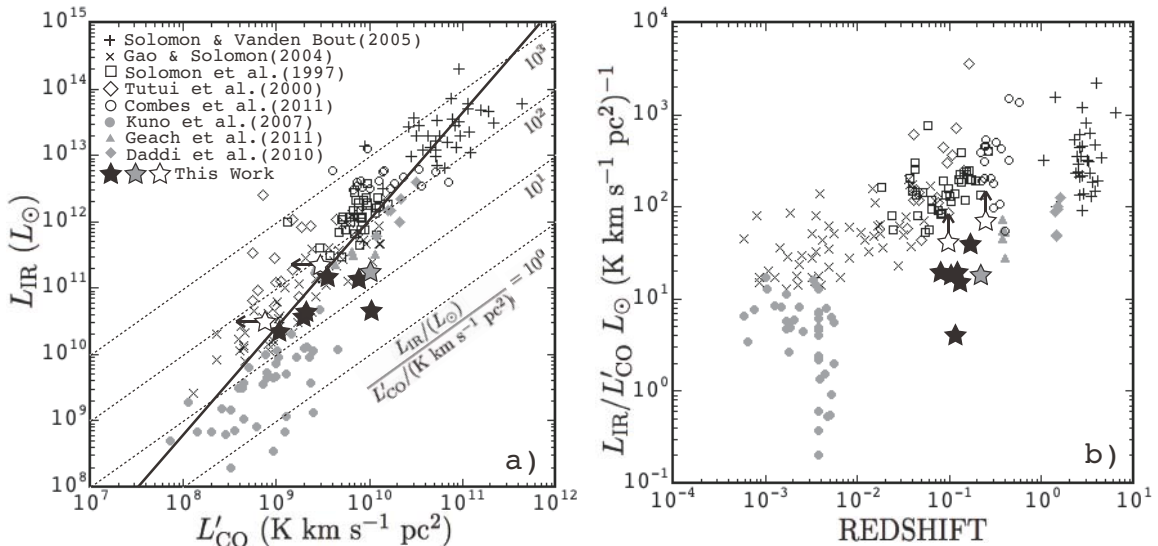


Figure 1: The black, gray and white stars in the plots represent the CO-detected galaxies ($S/N > 5$), the marginally CO-detected galaxies ($S/N \sim 4.4$) and not CO-detected galaxies ($S/N < 3$) in this work.

Structured Molecular Gas Reveals Galactic Spiral ArmsT. SAWADA^{1,2}, T. HASEGAWA², J. KODA³, T. HANDA⁴, M. SUGIMOTO^{1,2}¹ Joint ALMA Office, Chile.² NAOJ Chile Observatory, Chile.³ Stony Brook University, USA.⁴ Kagoshima University, Japan.

We have carried out survey observations toward the disk of the Milky Way (MW) in the ^{12}CO and ^{13}CO $J = 1-0$ lines using the Nobeyama Radio Observatory 45 m telescope. The line of sight at $l \approx 38^\circ$ samples the gas in both the Sgr arm and the inter-arm regions. The data reveal how the spatial structures in molecular gas vary across the spiral arms. We classify the molecular gas into two distinct components based on its appearance: the bright and compact (*structured*) component and the fainter and diffuse (i.e., spatially extended) component. The former is predominantly seen at the spiral arm velocities, while the latter dominates at the inter-arm velocities and is also found at the spiral arm velocities. We introduce the *brightness distribution function* (BDF) and the *brightness distribution index* (BDI, which indicates the dominance of the bright and compact component) in order to quantify the spatial structure of the gas. The radial velocities of BDI peaks coincide with those of high ^{12}CO $J = 3-2/J = 1-0$ ratio (i.e., warm/dense gas) and H II regions.

We then explore the development of structures in molecular gas in a much wider area of the MW disk, by applying the analysis of the BDF and BDI to the archival data from the Boston University–Five College Radio Astronomy Observatory ^{13}CO $J = 1-0$ Galactic Ring Survey. The structured molecular gas traced by higher BDI is located continuously along the spiral arms in the MW in the longitude–velocity diagram. This clearly indicates that molecular gas changes its structure as it flows through the spiral arms. Although the high-BDI gas generally coincides with H II regions, there is also some high-BDI gas with no/little signature of on-going star formation. These results support the possible evolutionary sequence; unstructured, diffuse gas transforms itself into structured state on encounter with the spiral arms, then star formation follows and eventually the gas returns to the unstructured state as it leaves the arms.

Disruption of Giant Molecular Associations by Shear Motion in the Spiral Galaxy M51Y. MIYAMOTO¹, N. NAKAI¹, AND N. KUNO²¹ Univ. of Tsukuba, Japan.² Nobeyama Observatory, Japan.

Understanding of the evolution of Giant Molecular Associations (GMAs) is important to improve our knowledge about massive star formation and galaxy evolution. We have investigated the dynamics of the molecular gas and the evolution of GMAs in the spiral galaxy M51 with the NRO 45-m telescope. The velocity components of the molecular gas perpendicular and parallel to the spiral arms were derived at each spiral phase from the distribution of the line-of-sight velocity of the CO gas. In addition, the shear motion in the galactic disk was determined from the velocity vectors at each spiral phase. It was revealed that the distributions of the shear strength and of GMAs are anti-correlation each other. This result suggests that the GMAs are destructed into GMCs by the strong shear, although surviving in the weak shear.

Kennicutt-Schmidt Law From Nearby Galactic Center to the Disk: On the Aspect of ^{13}CO

HSI-AN PAN^{1,2}, NARIO KUNO^{1,3}, AND AKIHIKO HIROTA⁴

¹ The Graduate University for Advanced Studies [SOKENDAI], Japan

² Nobeyama Observatory, Japan.

³ Nobeyama Observatory, Japan.

⁴ Nobeyama Observatory, Japan.

The star formation of galaxy is commonly expressed as Kennicutt-Schmidt Law (K-S Law), which relates the surface densities of molecular gas (Σ_{H_2}) and star formation rate (Σ_{SFR}) with the form of $\Sigma_{\text{SFR}} = A\Sigma_{\text{H}_2}^N$, where $N \approx 1.4$. Even though the physical processes leading to the K-S Law are not fully clear yet, the K-S Law has implied that the amount of molecular gas positively correlates with SFR. ^{12}CO has been widely used as a tracer of molecular gas owing to its high abundance and intensity. However, ^{12}CO suffers from the nature of optically thick. Thus it is worth seeking for an optically thin line, such as ^{13}CO and re-examining the K-S Law by determining the true mass of molecular gas. Since the sensitivity of NRO 45 m telescope has been improved, we made ^{12}CO (1–0) and ^{13}CO (1–0) spectral observation toward nearby spiral galaxy NGC 628 in 2012. In the preliminary results of NGC 628, surprisingly, the Σ_{H_2} derived from ^{13}CO positively relate to the Σ_{SFR} , while the correlation seems to be breakdown in ^{12}CO (Fig. 1). We then carried out the similar analysis with published data of the 45 m telescope of IC 342 (Hirota et al. 2010). For IC 342, the slope of K-S law appears to be changing among the center, bar, arm and inter arm regions of IC 342 (Fig. 2). Moreover, in both galaxies ^{12}CO overestimates the true mass of molecular gas. In poster, we discuss the possible reasons of the striking difference between the results of ^{12}CO and ^{13}CO for NGC 628 and the likely factors affecting the slope of the K-S plot in different galactic features of IC 342.

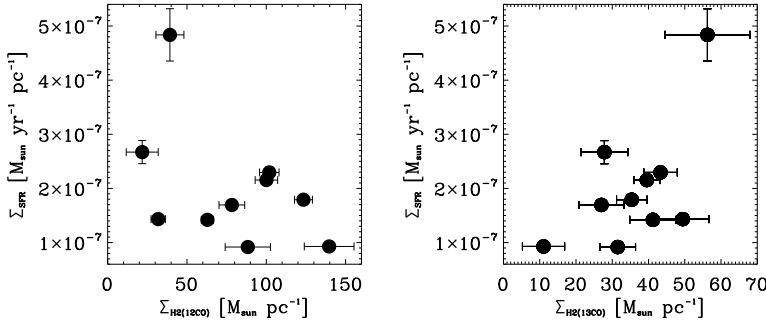


Figure 1: Preliminary results of NGC 628. The left and right panels show the K-S plot with molecular gas mass derived by ^{12}CO and ^{13}CO , respectively.

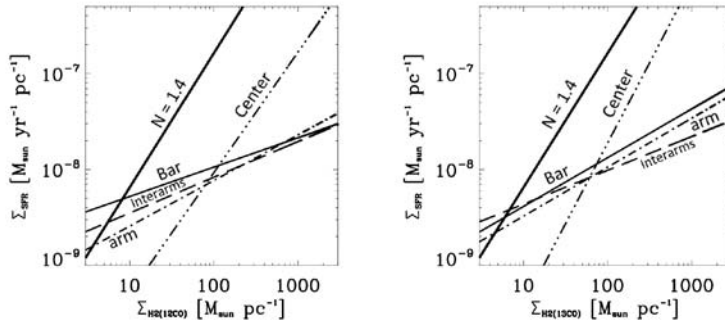


Figure 2: The K-S plot of IC 342. Here only shows the results of fitting, the complete results including the fitting of K-S Law and the observing data are shown in poster in color version. The left and right panels show the K-S plot with molecular gas content derived by ^{12}CO and ^{13}CO , respectively. The K-S plot with slope 1.4 is indicated to compare (with arbitrary constant A of K-S Law).

References:

Hirota, A., Kuno, N. et al. 2010, PASJ, 62, 1261

Feedback Mechanisms of Starbursts and AGNs through Molecular Outflows

S. MATSUSHITA¹

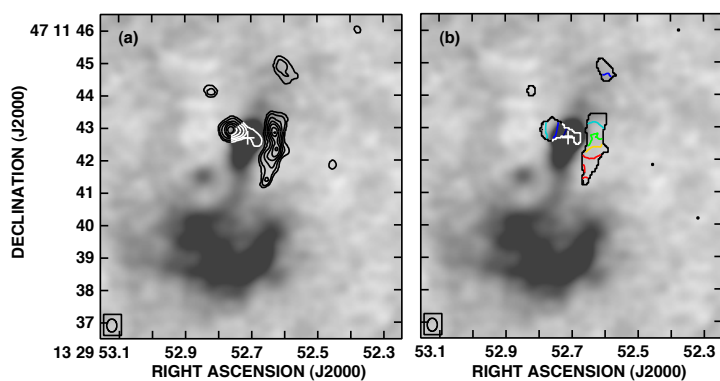
¹ Academia Sinica, Institute of Astronomy and Astrophysics (ASIAA), Taiwan.

I report our interferometric observations of molecular outflows from nearby starburst and Seyfert galaxies.

Molecular outflows and superbubbles from edge-on starburst galaxies we detected are large, around a few hundred pc to a few kilo-pc scales, but diffuse and weak. Since these features are located away from the galactic disks with systematic motion, it is rather easy to distinguish from the galactic (non-outflowing) disk gas. Since X-ray outflows are located inside of the molecular outflows or superbubbles with comparable or larger energies and pressures than those of molecular outflows, these indicate that the molecular outflows and superbubbles are pushed out by the X-ray outflows (Tsai et al. 2009, 2012). In M82, since the current starburst regions are located at the inner edge of the superbubble, we suggest that the expansion of the superbubble caused by the past starburst triggered the current starburst (Matsushita et al. 2000, 2005).

Molecular outflows from nearby Seyfert galaxies are much smaller, around ten-pc-scale, so high spatial resolution imaging is essential. Molecular outflows in Seyfert galaxies are located and moving along the AGN jets; in case of M51, molecular gas along radio jets has similar kinematics as ionized gas along the jets, suggesting that the molecular outflows are entrained by the AGN jets (Matsushita et al. 2007; see figures below). On the other hand, molecular gas near an AGN without jet does not show such feature, suggesting that the existence of the AGN jets affects the molecular gas structures around AGNs.

In both starburst and Seyfert galaxies, the strong activities affect the existing molecular gas that can be the fuel for the activities themselves. We may be observing the feedback mechanisms in starburst galaxies and AGNs.



Central $\sim 10''$ images of M51 CO(2-1) (a) integrated intensity and (b) intensity-weighted velocity field in contours. Greyscale image is the VLA 6 cm continuum emission (Crane & van der Hulst 1992). Cross indicates the location of the Seyfert 2 nucleus. Molecular gas at the western side of the nucleus is elongated along the radio jets with smooth velocity gradient (Matsushita et al. 2007).

References:

- Crane & van der Hulst 1992, AJ, 103, 1146
- Matsushita, S., et al. 2000, ApJ, 545, L107
- Matsushita, S., et al. 2005, ApJ, 618, 712
- Matsushita, S., Muller, S., & Lim, J., 2007, A&A, 468, L49
- Tsai, A.-L., et al. 2009, PASJ, 61, 237
- Tsai, A.-L., et al. 2012, ApJ, 752, 38

Boiling Molecular Cloud in the Central Molecular Zone

M. TSUBOI^{1,2}, M. T. SATO², K. TADAKI², A. MIYAZAKI³, AND T. HANDA⁴

¹ Institute of Space and Astronautical Science, Japan Aerospace Exploration Agency, Japan.

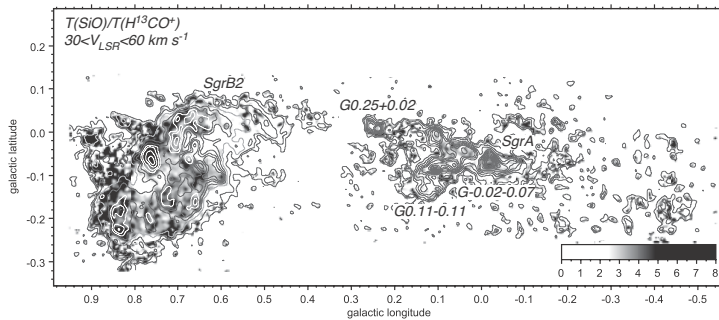
² Department of Astronomy, the University of Tokyo, Japan.

³ Korean VLBI Network, Korea Astronomy and Space Science Institute, Korea.

⁴ Graduate School of Science and Engineering, Kagoshima University, Japan.

The Central Molecular Zone (CMZ) (Morris and Serabyn, 1993) is a molecular cloud complex in the Galactic center region, which is the nearest central region of a spiral galaxy. This is the counterpart of a central molecular cloud condensation often observed in nearby spiral galaxies and containing molecular gas of several $10^7 M_{\odot}$ (e.g Tsuboi et al. 1999). We present results of a high-resolution wide-field mapping observation of the CMZ in SiO $v = 0, J = 2 - 1$ and $H^{13}CO^+ J = 1 - 0$ emission lines using the 25-beam receiver of 100 GHz band equipped in the Nobeyama Radio Observatory 45-m telescope (also see Tsuboi et al, 2011). The observations were performed during a survey program of the CMZ in order to explore molecular gas affected by shock in the regions and depict the high density molecular gas mass distribution.

There is a significant difference between the Sgr A and Sgr B2 complexes in $R = T(\text{SiO})/T(\text{H}^{13}\text{CO}^+)$. The Sgr B2 molecular cloud complex has several expanding shell-like structures. They have high ratio ($R > 8$) and very wide velocity width ($\Delta V > 50 \text{ km s}^{-1}$). On the other hand, there is no such high ratio area in the Sgr A complex although several expanding molecular shells are identified. Molecular cloud clumps are found using CLUMPFIND in the $H^{13}CO^+$ data cube and the clump mass functions (CMFs) are derived. The CMFs of the Sgr A and Sgr B2 complexes can be described by a similar power law (the power index is $\alpha \simeq -2$; $dN/dM \propto M^{\alpha}$) up to $M_{clump} < 1 \times 10^5 M_{\odot}$. In the higher mass range, although the CMF of the Sgr A complex still has the same power law, that of the Sgr B2 complex steepens rapidly. The origin of these expanding shells containing vast shocked molecular gas is still open. However, the properties of the shells may be a key information to understand active star formation in the central regions of galaxies.



The brightness temperature map (gray scale) of $T(\text{SiO})/T(\text{H}^{13}\text{CO}^+)$ in the CMZ. The velocity range is $30 < V_{\text{LSR}} < 60 \text{ km s}^{-1}$. The contours shows the distribution of SiO emission line. The Sgr B2 molecular cloud complex contains several shell-like structures with very high ratio (> 8).

References:

- Morris, M., Serabyn, E, 1996, ARAA, 34, 645
 Tsuboi, M. et al. 1999, ApJS, 120,1
 Tsuboi, M. et al. 2011, PASJ, 63, 763

ALMA Observations of the IR-bright Merger VV114

T.SAITO^{1,2}, D.IONO², M.YUN³, R.KAWABE^{2,4}, D.ESPADA², Y.HAGIWARA², M.IMANISHI²,
K.MOTOHARA¹, K.NAKANISHI², H.SUGAI², AND K.TATEUCHI¹

¹ University of Tokyo, Japan.

² National Astronomical Observatory of Japan, Japan.

³ University of Massachusetts, USA.

⁴ Joint ALMA Observatory, Chile.

The importance of galaxy mergers in the context of galaxy formation and evolution have been clearly demonstrated in various numerical simulations. The violent merger event not only results in large scale morphological transformation and mass accumulation, but it also triggers gas compression, turbulence, and gas inflow to the galactic center region. While our theoretical understanding has advanced significantly over the past few decades, observational studies have been hampered by the limit in sensitivity and resolution of the existing instruments.

Here, we present preliminary $^{12}\text{CO}(1-0)$, $^{13}\text{CO}(1-0)$, $^{12}\text{CO}(3-2)$, $^{13}\text{CO}(3-2)$, $\text{HCO}^+(4-3)$ and $\text{HCN}(4-3)$ maps of an IR-bright late stage merger VV114 obtained during cycle 0 of ALMA. This set of lines allow to probe the molecular gas distribution from the bulk of the gas to the denser and warmer components. The new data is more than an order of magnitude deeper than the past images, revealing detailed structure and tidal tails that were unseen before. The kinematical signature obtained from $^{12}\text{CO}(1-0)$ [beam size = $2.0'' \times 1.3''$] will be compared with the dense gas tracers in HCO and HCN lines, and will also be compared with star formation tracers and ages obtained through optical images.

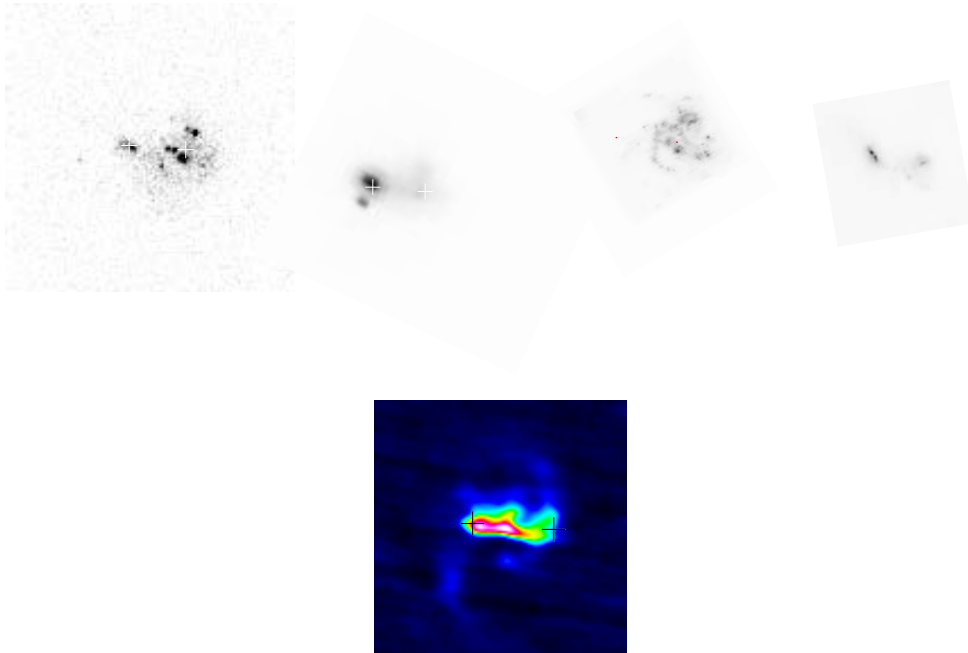


Figure 1: All annotations show the nuclei of each galaxies VV114E and VV114W. (Top Left) Chandra image finds extended X-ray emission. (Top Center-left) Spitzer/IRAC image. (Top Center-right) HST/STIS far UV image. (Top Right) HST/NICMOS image. (Bottom) ALMA $^{12}\text{CO}(1-0)$ integrated intensity image.

Interstellar dust properties of M51 from AKARI mid-infrared imagesF. EGUSA¹, T. WADA¹, I. SAKON², T. ONAKA², K. ARIMATSU^{1,2}, H. MATSUHARA¹¹ Institute of Space and Astronautical Science, Japan Aerospace Exploration Agency² Graduate School of Science, The University of Tokyo

Using mid-infrared (MIR) images of four photometric bands of the Infrared Camera (IRC) onboard the AKARI satellite, S7 (7 μm), S11 (11 μm), L15 (15 μm), and L24 (24 μm), we investigate the interstellar dust properties of the nearby pair of galaxies M51 with respect to its spiral arm structure. The arm region is defined by applying the wavelet analysis to a 3 μm image, which traces the stellar mass distribution. We measure a flux contrast between the defined arm and interarm regions for each band. The contrast is lowest (~ 2.4) in the S11 image, which is interpreted as this band best represents the total dust distribution including colder components, while the L24 image with the highest contrast (~ 3.1) traces warmer dust heated by star forming activities.

The surface brightness ratio between the bands, i.e. color, is measured over the disk of the main galaxy, M51a, at 300 pc resolution. We find that the distribution of S7/S11 is smooth and well traces the global spiral arm pattern while L15/S11 and L24/S11 peak at individual HII regions. Among many PAH band features in MIR, it is known that ionized PAHs are dominant carriers of the 7 μm feature while ionized and neutral PAHs both contribute to the 11 μm feature. The S7/S11 result thus indicates that the ionization state of PAHs is related to the spiral structure. However, the driving mechanism is not yet clear from currently available data sets. Comparison with observational data and dust models also supports the importance of the variation in the PAH ionization state within the M51a disk. Furthermore, existence of very small grains with high temperatures around bright HII regions and a higher PAH fraction to the total dust mass are suggested. Relationships between these dust properties and molecular and atomic gas distributions obtained from radio observations are also investigated.

Jet Kinematics and Absorbing Matter in the Quasar 1413+135

MINJU LEE, HARUKA HIWAKI, SEIJI KAMENO

We study the kinematics of jet of the radio-loud quasar 1413+135 based on the archival data from MOJAVE VLBA monitoring at $\lambda = 2$ cm. The quasar 1413+135 is known to have superluminal jets which have a knot that runs at the speed of $\beta_{\text{app}} = 1.8 \pm 0.2$ at maximum. We developed a simple analyzing tool for measuring the speed of jets. We found one jet component at apparent speed of $\beta_{\text{app}} = 1.29 \pm 0.13$ which was consistent with previous researches. The apparent speed yields the viewing angle and the minimum speed of $\theta \sim 38^\circ$ and $\beta_{\text{min}} = 0.79 \pm 0.12$, respectively. We also found the flux density variation which was possibly caused by surrounding materials in the vicinity of the nucleus. We consider that the flux density of the knot has increased as it escapes from the surrounding absorber.

ALMA cycle-0 observation of the Sombrero galaxy (M104)

A. DOI¹, K. HADA², K. KOHNO³, K. NAKANISHI⁴, Y. TERASHIMA⁵, T. KAWAGUCHI⁶,
S. SAWADA-SATOH⁷, K. AKIYAMA⁸, S. OZAKI⁹

¹ Japan Aerospace Exploration Agency, Japan

² Institute of Radio Astronomy of Bologna, Italy

³ The University of Tokyo

⁴ National Astronomical Observatory, Japan

⁵ Ehime University

⁶ University of Tsukuba

⁷ National Astronomical Observatory, Japan

⁸ The University of Tokyo

⁹ National Astronomical Observatory, Japan

The Sombrero galaxy is quite unique because of the nearest (9.3 Mpc) super massive black hole with $10^9 M_{\odot}$ as an extreme sub-Eddington and jet-suppressed accretion system. In the ALMA cycle-0, we have carried out point source photometry toward the Sombrero galaxy at (quasi-simultaneous) fifteen sideband frequencies in the band-3, 6, 7 and 9 to obtain continuum spectra for understanding of accretion and outflow phenomena in about 10 Schwarzschild radius or less. This is the most direct and promising approach to the vicinity of the event horizon, in advance of a future submm VLBI. We present a progress report of our study.

Search for Extragalactic H₂O Maser Toward Active GalaxiesY. HAGIWARA¹, A. DOI², K. HACHISUKA³¹ NAOJ, Japan.² ISAS/JAXA, Japan³ SHAO, China

The results of single-dish surveys for 22 GHz H₂O maser emission toward the nuclei of active galaxies using the Nobeyama 45-m telescope and Effelsberg 100-m telescope will be reported. The primary aim is a search for the H₂O maser in relatively nearby ($v_{sys} < 30,000$ km/s) narrow-line Seyfert 1 galaxies (NLS1s), which are known to have a smaller black hole mass than expected from M_{BH} - M_{Bulge} relations despite their luminosities being comparable to those of broad-line Seyfert 1 galaxies. The surveys were conducted with expectation that follow-up VLBI observation of the H₂O maser in NLS1 could prove a molecular gas disk and high mass accretion rate onto central engine in this particular type of galaxy. The observed galaxies were selected from radio-bright NLS1s detected in the NVSS survey at either 1.4 GHz or 5 GHz. In these surveys, no new H₂O maser has been detected at luminosity upper limit of $< 5 L_{\odot}$, confirming that strong H₂O masers are not associated with the nuclei of NLS1s. The nature of the known H₂O maser in NLS1s will be discussed by using, for example, the correlation between radio and H₂O maser luminosity.

$^{12}\text{CO}(J=1-0)$ Survey with NRO 45 m of GOALS Luminous Infrared Galaxies: Star Formation Efficiency against Galactic Merger and AGN Activity

T. YAMASHITA^{1,2}, S. KOMUGI³, H. MATSUHARA¹, H. INAMI⁴, L. ARMUS⁵, S. STIERWALT⁵,
K. KOHNO⁶, D. IONO³, K. ARIMATSU¹

¹ Institute of Space and astronomical Science, Japan Aerospace Exploration Agency

² Department of Physics, Tokyo Institute of Technology

³ National Astronomical Observatory of Japan

⁴ National Optical Astronomy Observatory

⁵ Spitzer Science Center, California Institute of Technology

⁶ Institute of Astronomy, The University of Tokyo

We present the results of the survey of $^{12}\text{CO}(J=1-0)$ from nearby luminous infrared galaxies (LIRGs: $L_{\text{IR}} > 10^{11} L_{\odot}$) with Nobeyama 45 m telescope. This survey has been conducted to investigate star formation activities in LIRGs, providing their molecular gas mass. The star formation efficiency (SFE) on average is comparable to typical ones of normal galaxies and giant molecular clouds in Milky Way. The SFE has no correlations with the galactic merger stages and the active galactic nuclei (AGN) activity.

The nuclear activities in the nearby LIRGs are various such as violent star-forming or AGN. The morphology of the nearby LIRGs range from isolated galaxies or the early stage to the final stage of the galaxy-galaxy merger/interaction, which can trigger starburst events. Understanding the star formation and the evolution of local LIRGs need to investigate how the energy sources and the merger stages relate to the IR emission or the star formation. The Great Observatory All-sky LIRG survey (GOALS) is a project to reveal the true character of nearby LIRGs by combining multi-wavelength imaging and spectroscopic data. The samples of this survey are an unbiased subset of LIRGs in the GOALS project.

We obtained the molecular gas mass M_{H_2} in nearby 39 LIRGs by using the $^{12}\text{CO}(J=1-0)$ emission line. We found that these nearby LIRGs have M_{H_2} of $2.9 \times 10^9 - 9.9 \times 10^{10} M_{\odot}$. The CO luminosity have a correlation with the IR luminosity L_{IR} , scaled to a $15''$ beam of the CO observation. The average SFE inferred from $L_{\text{IR}}/M_{\text{H}_2}$ is $0.62 \pm 0.44 \text{ Gyr}^{-1}$, which is about 10 times lower than the nearby ULIRGs' typical SFE and is comparable to the SFE of local normal galaxies and giant molecular clouds in Milky Way. $L_{\text{IR}}/M_{\text{H}_2}$ is compared with the merger stages classified by their morphologies of the optical images (Figure A), and with $6.2 \mu\text{m}$ polycyclic aromatic hydrocarbon equivalent width (PAH EQW), which indicates AGN contribution to Mid-IR emission (Figure B). There are no correlation between both. The SFE of nearby LIRGs may be independent on the presence of AGN and the phases of mergers, and the stars are being formed with a roughly the same and moderate efficiency; although some uncertainties from the beam aperture, the merger classification or a CO- H_2 conversion factor are remained.

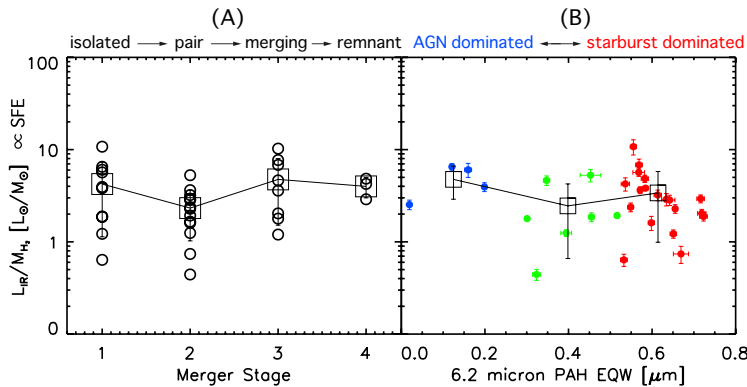


Figure: (A) The star formation efficiency (SFE) of nearby LIRGs at each merger stages. (B) The SFE vs. $6.2 \mu\text{m}$ PAH EQW which is an indicator of AGN activities on Mid-IR.

Nobeyama 45 m Telescope Legacy Project: Line Survey of Galaxies

T. NAKAJIMA¹, S. TAKANO^{2,3}, K. KOHNO⁴, AND THE LINE SURVEY TEAM

¹ Solar-Terrestrial Environment Laboratory, Nagoya University, Japan.

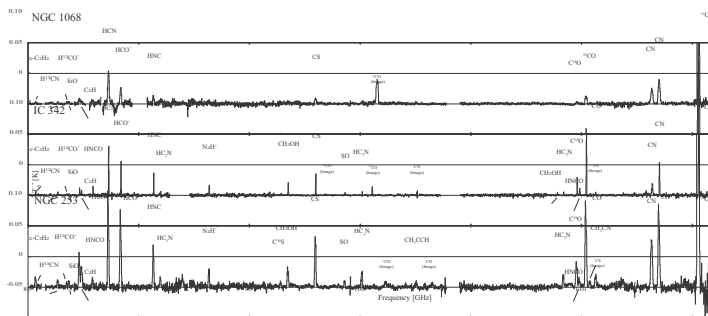
² Nobeyama Radio Observatory, National Astronomical Observatory of Japan.

³ The Graduate University for Advanced Studies (SOKENDAI), Japan.

⁴ Institute of Astronomy, University of Tokyo, Japan.

To date, about 40 molecular species have been identified in nearby external galaxies. As a result, it is now possible to study molecular abundances and chemical reactions in external galaxies. In fact, some groups have suggested that it is possible to diagnose power sources in dusty galaxies using molecular line ratios (e.g., [1-6]). The observations of the molecular gas chemistry of the active galactic nucleus (AGN) toward NGC 1068, one of the nearest galaxies with an AGN, have been reported by [2, 7-8]. However, further systematic observations of molecular lines are indispensable to study the impact of AGN on the interstellar medium. Therefore, we started a project to conduct a line survey in the 3-mm band of NGC 1068 using the new receiver in the 45-m telescope at Nobeyama Radio Observatory [9]. The beam size of this telescope (18'' at 86 GHz) is smaller than the size of the circumnuclear starburst ring in NGC 1068 ($d \sim 30''$), and it is therefore essential to study the impact of the AGN on the surrounding molecules; this will enable us to mitigate the contamination of the molecular lines from the circumnuclear starburst region in NGC 1068. We also observed NGC 253 and IC 342 to compare the effects of AGN and starburst on molecular abundance.

The observations at the 3 mm region (85–116 GHz) were carried out in 2009–2011. We successfully detected cyclic- C_3H_2 ($J_{Ka,Kc} = 2_{1,2}-1_{0,1}$), C_2H ($N = 1-0$) and $H^{13}CN$ ($J = 1-0$) for the first time in NGC 1068 [10]. We are also detected $H^{13}CO^+$, SiO, HCN, HCO^+ , HNC, HC_3N , CH_3OH , CS, SO, ^{13}CN , $C^{18}O$, HNCO, ^{13}CO , CH_3CN , CN and ^{12}CO in NGC 1068. We obtained the abundances C_2H and cyclic- C_3H_2 relative to CS. As a result, we found no significant differences in the relative abundances between NGC 1068 and NGC 253. This result suggests that the basic carbon-containing molecules are either insusceptible to AGN, or are tracing cold ($T_{rot} \sim 10$ K) molecular gas rather than X-ray irradiated hot gas. Moreover, we found low intensity ratios of N_2H^+ and CH_3OH relative to ^{13}CO and high ratios of CN, HCN and $H^{13}CN$ in NGC 1068 as compared with NGC 253 and IC 342. CN and HCN molecules are considered to be the X-ray tracers in theory.



The composite line spectra toward NGC 1068 (upper), IC 342 (center) and NGC 253 (lower). The intensity scale is in T_A^* .

References:

- [1] Kohno, K., et al. 2001, ASP Conf., 249, 672, [2] Usero, A., et al. 2004, A&A, 419, 897, [3] Kohno, K. 2005, AIP Conf., 783, 203, [4] Imanishi, M. et al. 2007, AJ, 134, 2366, [5] Kohno, K. et al. 2008, Ap&SS, 313, 279, [6] Krips, M. et al. 2008, ApJ, 677, 262, [7] Pérez-Beaupuits, J. P. et al. 2009, A&A, 503, 459, [8] García-Burillo, S. et al. 2010, A&A, 519, 2, [9] Nakajima, T. et al. 2008, PASJ, 60, 435, [10] Nakajima, T. et al. 2011, ApJ, 728, L38

**Star-formation types and molecular gas in nearby spiral galaxy NGC 253:
suggestion for high-redshift star-formation activities**

K. NAKANISHI¹, K. SORAI², N. KUNO³, T. TOSAKI⁴, K. KOHNO⁵, AND N. NAKAI⁶

¹ National Astronomical Observatory of Japan, Japan.

² Hokkaido University, Japan.

³ Nobeyama Radio Observatory, Japan.

⁴ Joetsu University of Education, Japan.

⁵ University of Tokyo, Japan.

⁶ Tsukuba University, Japan.

Recent observations are confirming existence of two different star-formation types in both low-redshift and high-redshift galaxies. One is a long-lasting mode for star-formation in galactic disks ('disk'), and the other is a more rapid mode for starbursts ('starburst'). Those can be recognized from a fact that 'starburst' galaxies and 'disk' star-forming galaxies occupy distinct regions in the gas mass versus star-formation rate plane (e.g. Daddi et al. 2010). Origins and mechanisms of these two different star-formation types are, however, still under discussion.

We investigate differences between 'disk' and 'starburst' star-formation based on NGC 253 observation data. NGC 253 is a well-studied nearby barred-spiral galaxy. This galaxy is known as nearest and prototypical starburst; the strong infrared emission stands for a fact that intense massive star-formation activity has been taking place in the central region of this galaxy. NGC 253 also has disk star-formation; star-forming regions spread on its disk region and mainly associate to the "2-kpc ring". NGC 253 provides us unique opportunity to look into detail of the two star-formation types. We have already obtained ¹²CO molecular emission line maps which cover both central region and disk region of NGC 253 using the Nobeyama 45-m radio telescope and the Atacama Submillimeter Telescope Experiment. Those maps show distributions of molecular gas and also enable us to obtain physical properties of molecular gas. Furthermore, thanks to recently obtained high-quality satellite-based ultraviolet and infrared data, we can assess precisely not only star-formation rate but also interstellar extinction (A_V) within the galaxy. Combining those data, we can discuss differences of characteristics between 'starburst' and 'disk' star-formation in spatial resolutions of less than 500 pc.

Our findings are as follows. 1) Star-formation rate to molecular gas mass ratios of the central region and the disk region mostly correspond to those of 'starburst' and 'disk'. Then we can assume that the central region and disk star-forming regions can represent 'starburst' and 'disk', respectively. 2) CO-to-H₂ conversion factor (X_{CO}) for the central region molecular gas is about three times smaller than that for the disk region gas. 3) Beam averaged molecular gas volume density in the central region is about ten times higher than that in the disk region. This is as expected and suggest that different initial mass function is not necessary for the 'starburst'. 4) Average ¹²CO(3-2) to (1-0) line ratios for the central region and the disk region are 0.9 and 0.5, respectively. These values would be references for high-redshift galaxies observations.

Distributions of Dusty Star Forming Region in Local Starburst Galaxies

K. TATEUCHI¹, K. MOTOHARA¹, M. KONISHI¹, H. TAKAHASHI¹, N. KATO¹, Y. KITAGAWA¹, Y. YOSHII¹, M. DOI¹, K. KOHNO¹, K. KAWARA¹, M. TANAKA¹, T. MIYATA¹, T. TANABE¹, T. MINEZAKI¹, S. SAKO¹, T. MOROKUMA¹, Y. TAMURA¹, T. AOKI¹, T. SOYANO¹, K. TARUSAWA¹, S. KOSHIDA¹, T. KAMIZUKA¹, K. ASANO¹, M. UCHIYAMA¹, K. OKADA¹, AND T. HANDA²

¹ Institute of Astronomy, the University of Tokyo, Japan

² Kagoshima University, Japan

In recent years, many large deep cosmological surveys have revealed that the star forming rate (SFR) density of the universe (cosmic SFR density) increases by an order of magnitude from the present to $z \sim 1$. The densities at high redshifts are dominated by infrared bright galaxies, especially Luminous Infrared Galaxies (LIRGs; $L_{IR} = L [8-1000 \mu\text{m}] = 10^{11}-10^{12} L_{\odot}$) and Ultra Luminous Infrared Galaxies (ULIRGs; $L_{IR} = 10^{12}-10^{13} L_{\odot}$) (e.g., Goto et al. 2010). Their IR emission is thermal dust emission in the mid-IR (MIR) to far-IR (FIR) wavelength caused by absorbing UV photons from intensive star formation and/or luminous active galactic nuclei (AGNs). In order to know the detailed properties of these galaxies, and to understand how they are formed and evolved, local U/LIRGs are ideal laboratories for spatially resolved star-formation processes. However, U/LIRGs are affected by a large amount of dust extinction ($A_V > 3$ mag for LIRGs; Alonso-herrero et al. 2006), produced by their star formation activities. Then, hydrogen Pa α ($1.8751 \mu\text{m}$) represents a nearly unbiased tracer of the ongoing obscured SFR by its strength and relative insensitivity to the extinction. However, due to poor atmospheric transmittance around that wavelength, ground-based observations of Pa α have been difficult so far.

ANIR is a near infrared camera for the University of Tokyo Atacama 1.0m telescope (miniTAO), installed at the summit of Co. Chajnantor (5640m altitude) in northern Chile (Yoshii et al. 2010). The high altitude and extremely low precipitable water vapor (PWV=0.5mm) of the site enable us to perform observations of Pa α . The first light observation was carried out in July 2009, and Pa α images have been successfully obtained using $N1875$ and $N191$ narrow-band filters. Galaxies listed in the catalog of IRAS-RBGS were drawn using a criteria with a velocity of recession of $2800 \text{ km/s} \sim 8100 \text{ km/s}$ and $4.5 \times 10^{10} < L_{IR}(8-1000 \mu\text{m}) [L_{\odot}] < 6.5 \times 10^{11}$. In total, 38 objects were observed with $N191$ (for redshifted Pa α), and H and K_s broad-band filters (for continuum) in June 2009–October 2011 (5 observation runs).

To quantify the morphology of local LIRGs, concentration index (Conselice et al. 2003) is used. The definition is $C = 5 \log (r_{80}/r_{20})$, where r_{80} and r_{20} are the radii which contain 80% and 20% of the total flux, respectively. The total flux is defined as a flux contained within 1.5 times the Petrosian radius. We estimated C-Index for Pa α line images (C_L ; star-forming) and $1.9 \mu\text{m}$ continuum images (C_C ; stellar population). Our result shows quantitatively that there are two types of star-forming region profile of LIRGs (Figure 1). These facts suggest that the origin of the two star-forming modes is due to the difference in star forming process; Group-A is in the minor merging mode in which gas falls into center of elliptical-galaxy like potential, while Group-B is in the major merger mode.

In order to understand the details of the origin of these two modes, it is necessary to observe these galaxies which are classified into the two star-forming modes respectively by using CO($J = 1 - 0$) emission line that can reveal the gas mass, the morphology of gas, and the gas motion.

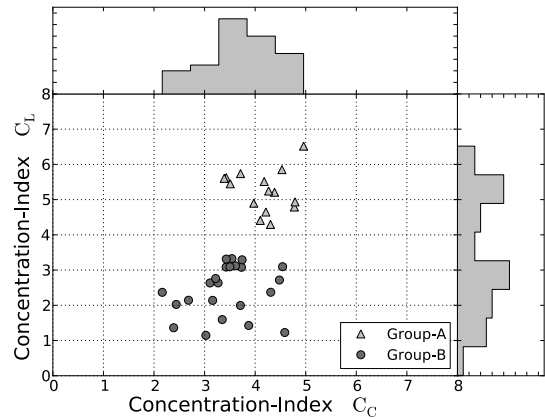


Figure 1: Comparison of C_L and C_C , where a bimodal distribution of Pa α profile is seen.

**NRO M33 All-Disk Survey of Giant Molecular Clouds (NRO MAGiC):
Properties of Giant Molecular Clouds in M33**

SACHIKO ONODERA¹, NARIO KUNO^{2,3}, TOMOKA TOSAKI⁴, KAZUYUKI MURAOKA⁵, RIE MIURA⁶,
KOTARO KOHNO^{6,7}, KOUICHIRO NAKANISHI^{3,8}, TSUYOSHI SAWADA⁹, SHINYA KOMUGI⁹,
HIROYUKI KANEKO¹⁰, AKIHIKO HIROTA², AND RYOHEI KAWABE^{2,9}

¹Meisei University, Japan

²Nobeyama Radio Observatory, National Astronomical Observatory, Japan

³The Graduate University for Advanced Studies (Sokendai), Japan

⁴Joetsu University of Education, Japan

⁵Osaka Prefecture University, Japan

⁶Institute of Astronomy, The University of Tokyo, Japan

⁷Research Center for the Early Universe, University of Tokyo, Japan

⁸ALMA Project Office, National Astronomical Observatory, Japan

⁹Joint ALMA Office, Chile

¹⁰The University of Tsukuba, Japan

We report the results of our observations of the ^{12}CO ($J=1-0$) line emission in the Local Group galaxy M33. The observations have been conducted as part of the Nobeyama Radio Observatory M33 All-disk survey of Giant Molecular Clouds project (NRO MAGiC). The spatial resolution is 80 pc and the velocity resolution is 2.5 km/s. We identified 74 major giant molecular clouds (GMCs) within the galactocentric distance of 5.1 kpc. We present the GMC properties of size, velocity width, mass, degree of virialization, star formation rate, association of young clusters, and show discussions on them.

Molecular Gas and Star formation in Giant HII regions of M33

T. TOSAKI¹, R. MIURA², K. KOHNO³, N. KUNO⁴, S. ONODERA⁵, AND MAGIC TEAM

¹ Joetsu University of Education

² National Astronomical Observatory of Japan, ³ University of Tokyo, ⁴ Nobeyama Radio Observatory, ⁵ Meisei University

We have extensively studied the properties of molecular clouds which are associated with the supergiant HII region NGC 604 in the nearest ($D = 840$ kpc) spiral galaxy M33.

Massive star formation process in galaxies is one of unresolved important issues in recent galactic astronomy, because it governs the energy budget of galaxies as well as chemical evolution of galaxies. Despite of its importance, however, the formation process of massive stars remains unclear. In some galaxies there exist giant/supergiant HII regions (hereafter referred to as GHRs). GHRs have high $H\alpha$ luminosities of $\sim 10^{40}$ ergs s^{-1} , which corresponds to \sim a few 100 O5 stars and provide us with an ideal environment to understand the clustered OB star formation process and their impact on the ambient interstellar medium (ISM). In other words, GHR can be “mini-starburst”, therefore, understanding the star formation process in these GHRs will be also important to study starburst phenomena in various galaxies. These GHRs are also crucial in the evolution of starburst in galaxies.

NGC 604 is the largest super GHR in M33 accompanied with massive molecular clouds and the central OB star cluster. Based on our results, we suggest that giant molecular cloud complex associated with NGC 604 is a unique laboratory for different, especially, for the early and intermediate stages along evolutionary path of star formation in the GHR (e.g. Tosaki et al. 2007, Miura et al. 2010). Then, the next questions are the internal structure of each GMCs and the variation of physical and chemical properties of dense molecular gas along evolutionary path of star formation.

We will discuss about the properties of molecular gas and star formation in the GHRs of M33.

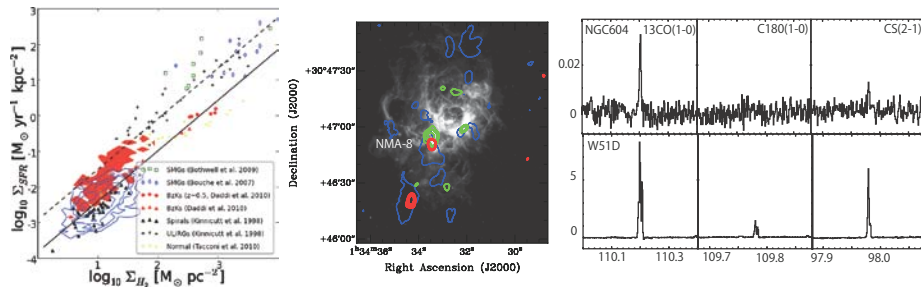


Figure 1: (left) The correlation between the surface densities of molecular gas (Σ_{H_2}) and the Star Formation Rate for GHRs (red filled contour) and for non-GHRs (blue contour) in M33, compared with that of other galaxies (Miura 2012). Data plots of other galaxies and lines are quoted from Daddi et al. (2010). The lower solid line is “Sequence of Disks”, and the upper dashed line is “Sequence of starburst”. We see that the plots for GHRs reach the “Sequence of starburst”. (middle) The $^{12}\text{CO}(1-0)$ (blue), HCN (red), 90 GHz (green) continuum superposed on $H\alpha$ emission (Miura et al. 2010). (right) The $^{13}\text{CO}(1-0)$, $\text{C}^{18}\text{O}(1-0)$, and $\text{CS}(2-1)$ emission toward NMA-8 in NGC 604 (top) and W51D, an active star forming region in our Galaxy (bottom). We find significant decrease of C^{18}O with respect to CS in NMA-8 as well as in the center of W51D, despite the fact that we see rather normal $^{13}\text{CO}/\text{CS}$ ratios in these.

References:

- Daddi et al. 2010, ApJ, 714, L118
 Miura, R.E., 2012, PhD thesis, University of Tokyo
 Miura et al., 2010, ApJ, 724, 1120
 Tosaki et al 2007, ApJL, 664, L27

Spectroscopic Observations of YSOs in the Magellanic Clouds: Current and Future Studies

T. SHIMONISHI¹, T. ONAKA², I. SAKON², Y. ITA³, A. KAWAMURA⁴, H. KANEDA⁵

¹Department of Earth and Planetary Sciences, Graduate School of Science, Kobe University

²Department of Astronomy, Graduate School of Science, The University of Tokyo

³Astronomical Institute, Graduate School of Science, Tohoku University

⁴National Astronomical Observatory of Japan

⁵Graduate School of Science, Nagoya University

Chemical diversity of materials that forms stars and planets in the universe is one of the great interests of present-day astronomy. Star-/planet-formation activities can occur in various kinds of galaxies which differ in many ways such as size, shape, and environment. Thus it is important to understand how galactic characteristics affect the properties of materials around YSOs.

The Large and Small Magellanic Clouds are the nearest low-metallicity galaxies to our Galaxy (~50 kpc for LMC, and ~60 kpc for SMC). There are two main reasons to study YSOs in the Magellanic Clouds. First, YSOs in the Magellanic Clouds enables us to investigate how the different metallicity environments affect the properties of circumstellar materials. Metallicities of the LMC and the SMC are known to be approximately 1/2 and 1/5 compared to the solar neighborhood. Chemical evolution of the universe is, as a first-order approximation, the evolution of metallicity. In this respect, it is especially important to investigate YSOs in low-metallicity environments. Next, YSOs in the Magellanic Clouds enables us to investigate the properties of circumstellar materials by comparison with luminosity of the source thanks to their well-determined distances. Also, the face-on geometry of the LMC allows us to two-dimensionally compare the distribution of YSOs and the ISM. The above points are great advantages compared to observations of Galactic YSOs.

For the last few years, it has been pioneer days for spectroscopic studies of YSOs in the Magellanic Clouds. A number of embedded YSOs are spectroscopically identified in the LMC and SMC with *AKARI*, and their near-infrared ice features are discussed in detail. In addition, a large number of YSOs are also identified by the *Spitzer* observations, and mid-infrared ice features are investigated. Ices are considered to be a major reservoir of molecules such as water, carbon dioxide, and various organic compounds that are essential for the presence of life. We are going to discuss the properties of circumstellar ices around high-mass YSOs in the LMC and SMC based on infrared spectroscopic data. It is shown that ices around YSOs in the Magellanic Clouds possess different properties in terms of molecular abundances and column densities. The effect of galactic metallicity on the ice chemistry will be discussed in the presentation.

For the future, it is very interesting to focus on gas-phase species in circumstellar environments of Magellanic YSOs. Since sublimation of ices significantly affect the gas-phase chemistry, the unique ice chemistry in the Magellanic Clouds possibly affect gas-phase species. Thus interferometric observations of Magellanic YSOs should be one of the new trends in radio astronomy in the ALMA era. We also discuss the future possibilities of radio observations toward YSOs in extragalaxies.

X-ray irradiated dense molecular medium in the active nucleus of NGC 1097

T. IZUMI¹, K. KOHNO¹, S. MARTIN², K. SHETH³, S. MATSUSHITA⁴, D. ESPADA⁵
AND NGC1097 COLLABORATORS

¹ Institute of Astronomy, The University of Tokyo

² European Southern Observatory

³ National Radio Astronomy Observatory

⁴ Academia Sinica Institute of Astronomy and Astrophysics

⁵ National Astronomical Observatory of Japan

Investigation of dense molecular gas plays a key role in studying the nature of the dominant source of energy in galaxies such as active galactic nuclei (AGN) and starbursts. It is expected that the various heating mechanisms will produce different signatures in the molecular properties, e.g., photodissociation regions (PDRs) caused by intense UV radiation from massive stars and X-ray dominated regions (XDRs) formed near the very center of AGN^{*1,2,3}. Cosmic rays from supernovae (SNe) and the injection of mechanical energy induced by the AGN jet or SNe (mechanical heating) are also important^{*4,5}. To diagnose these energy sources by mm/submm spectroscopic observation is essential for the investigation of buried AGNs in dusty nuclei because these wavelengths do not suffer from dust extinction.

On the basis of these interests, many “key molecules” have been identified and proposed as a useful diagnostic tool for the dense interstellar medium (ISM) in galaxies by mm/submm spectroscopic observations. Among them, we have identified HCN enhancement with respect to HCO⁺ and CO as the most promising indicator of the buried AGN^{*6,7,8,9}. Also, some theoretical models predict high HCN abundance^{*2,3,10}. However, some Seyferts do not show this enhancement possibly due to the lack of spatial resolution, i.e., low spatial resolution spectral surveys can not resolve the inner central structure of nearby active galaxies, where both AGN and starburst often coexist within a few 100 pc scales. Therefore, one may observe a mixture of dense molecular clouds with different physical and chemical properties. Clearly, interferometric high spatial resolution observations are needed.

Therefore, we have conducted an observation towards the nucleus of a type-1 Seyfert, NGC 1097 ($L_{2-10\text{keV}} = 3.7 \times 10^{40} \text{ erg s}^{-1}$ ^{*11}), in ALMA Cycle 0^{*12} at Band 7. The array configuration was a compact one with 16 antennas, and the resulting spatial resolution was $\sim 1''.5 \times 1''.2$. We achieved r.m.s. noise level of $\sim 2 \text{ mJy}$ (velocity resolution is $\sim 8 \text{ km/s}$) with the on-source time of only $\sim 1 \text{ hr}$. The results of this observations are summarized as follows. (1) We detected the strong HCN(J=4-3) emission and the HCN/HCO⁺ line ratio is over 1, which is a similar value to the low-J results. (2) The most surprising result is an extremely high HCN(J=4-3)/CS(J=7-6) line ratio, which is over 10. A similar ratio (~ 30) is also found in the luminous AGN galaxy, NGC 1068. However, these extremely high line ratios have never been observed in starburst galaxies and star-forming regions (e.g., ~ 3.5 in NGC 253^{*13,14} and ~ 1.7 in Ori-KL^{*15}). (3) No vibrationally excited HCN emission, HCN($v_2=1$, J=4-3) has been detected in this galaxy, whose nucleus is not IR luminous. However, strong HCN($v_2=1$, J=4-3) emission has been reported in the IR luminous galaxy, NGC 4418^{*16}. This indicates that the amount of the HCN($v_2=1$, J=4-3) might simply depend on IR luminosity.

Considering these results, we conclude that the HCN abundance is strongly enhanced in the nucleus of NGC 1097 and the HCN/CS line ratio is a very effective discriminator between AGN and starburst.

References:

- ^{*1} Maloney et al. 1996, ApJ, 466, 561 ^{*2} Meijerink & Spaans. 2005, A&A, 436, 397 ^{*3} Meijerink et al. 2007, A&A, 461, 793 ^{*4} García-Burillo et al. 2010, A&A, 519, 2 ^{*5} Meijerink et al. 2011, A&A, 525, 119 ^{*6} Kohno et al. 2001, ASPC, 249, 672 ^{*7} Kohno et al. 2005, AIPC, 783, 203 ^{*8} Krips et al. 2008, ApJ, 677, 262 ^{*9} Davies et al. 2012, A&A, 537, 133 ^{*10} Harada et al. 2010, ApJ, 721, 1570 ^{*11} Iyomoto et al. 1996, PASJ, 48, 231 ^{*12} Kohno et al. 2011.00180S ^{*13} Bayet et al. 2009, ApJ, 707, 129 ^{*14} Knudsen et al. 2007, ApJ, 666, 156 ^{*15} Schilke et al. 1997, ApJS, 108, 301

Wide-field ^{12}CO (J=1–0) imaging of the nearby barred galaxy M83 with the NMA and the 45m telescopeA. HIROTA¹, N. KUNO^{1,2}, A. TANAKA³ H. NAKANISHI⁴ R. KAWABE⁵¹ Nobeyama Radio Observatory, .² Nobeyama Radio Observatory, The Graduate University of Advanced Studies (SOKENDAI).³ Faculty of Science, Kagoshima University,⁴ Faculty of Science, Kagoshima University,⁵ Joint ALMA Observatory,

We present results of the mapping observations of the nearby barred spiral galaxy M83 in ^{12}CO (1–0) carried out with the Nobeyama Millimeter Array (NMA). To correct for the lack of sensitivity to diffuse emission, the interferometric data are combined with the data taken with the Nobeyama 45m telescope. Target field of the observations consists of 46 pointings and covers the entire extent of the molecular bar and part of the spiral arms. Galactic structures are resolved with a spatial resolution of $\sim 100 \text{ pc} \times 200 \text{ pc}$ and several inter-arm clouds are also detected.

'Classic' density wave theory along with the galactic shock model predict that galactic structures will organize the progress of star formation (SF) through agglomeration and compression of molecular material. In this picture, distribution of molecular clouds (MCs) and young stellar populations should show a rather coherent pattern which goes from upstream to downstream on the rotating frame. However, in recent, some observational evidences against this rather simple picture have been reported (e.g, Foyle+11), and the picture of persistent galactic structures, which is a starting point of 'classic' density wave theory, is also been attacked by numerical simulations (e.g., Wada+11). Re-examination of the relation between MCs and SF regions are thus highly required. Barred galaxies offer a unique opportunity in that it is known to show a variety of star forming activity within a single galaxy.

Here, taking advantage of the spatial resolution and sensitivity to the diffuse gas clouds, relations between molecular gas and star forming regions are examined to see whether galactic structures in the inner disk of M83 exert influences on progress of star formation. Two characteristics are found with the combined (NMA+45m) data: 1) star formation efficiency (SFE) is found to be lower by about factor of two inside the bar compared to outside of the bar, and 2) young star forming regions tends to be preferentially located at the leading side of gas clouds, at least within the bar and near both ends of the bar. Gas kinematics are representative of non-circular motion induced by the 'slowly' rotating bar. The bar-induced kinematics of molecular clouds is likely to be responsible for the SF characteristics: short dynamical time scale within the bar, which is comparable to the life time of GMC, suppress the SFE within the bar, and the large relative velocities between MCs and underlying stellar bar due to the slow pattern speed give rise to the moderately organized pattern of star formation.

Expected Observations of Star Formation Process: from Molecular Cloud Core to Protostar Phase

KOHI TOMISAKA^{1,2}, AKIMASA KATAOKA², KENGO TOMIDA³, AND MASASHIRO N. MACHIDA⁴

¹ NAOJ, Japan.

² Astron. Dept., Graduate Univ. for Advanced Studies (SOKENDAI), Japan.

³ Astron. Dept., Princeton U., USA

⁴ Kyushu U., Japan

We did MHD simulations of the contraction of rotating, magnetized molecular cloud cores. In the molecular cores, B-field and angular momentum (J) vector are not always aligned. When a first hydrostatic core forms, axisymmetric structure appears and average B and J are parallel in small scale. However, in large scale, the configuration is far from this. This means that contraction process is imprinted on the snapshot. We calculated two mock observations of MHD simulations

1. the polarization from thermal dust emission to reveal the magnetic evolution (Kataoka et al. 2012; Shinnaga et al. 2012; Tomisaka 2011) and
2. the line emissions from interstellar molecules to reveal the evolution of density and velocity (Tomisaka and Tomida 2011; Tomida et al 2011).

Comparing the mock observations with true ones, we can answer several questions: in which case the hourglass-shaped and S-shaped magnetic fields are seen; how the distribution of polarized intensity is understood; how the first hydrostatic core should be observationally identified.

References:

Kataoka, A., Machida, M.N., Tomisaka, K. 2012, submitted to ApJ

Shinnaga, H. et al. 2012, ApJL 750, L29

Tomida, K., Machida, M.N., Saigo, K., Tomisaka, K., Matsumoto, T. 2011, ApJL 725, L239

Tomisaka, K. 2011, PASJ, 63, 715

Tomisaka, K., Tomida, K. 2011, PASJ 63, 1151